

Catalysis Science & Technology

Accepted Manuscript



This article can be cited before page numbers have been issued, to do this please use: X. Zhu, P. Wang, M. Li, Q. Zhang, E. A. Rozhkova, X. Qin, X. Zhang, Y. Dai, Z. Wang and B. Huang, *Catal. Sci. Technol.*, 2017, DOI: 10.1039/C7CY00393E.



This is an Accepted Manuscript, which has been through the Royal Society of Chemistry peer review process and has been accepted for publication.

Accepted Manuscripts are published online shortly after acceptance, before technical editing, formatting and proof reading. Using this free service, authors can make their results available to the community, in citable form, before we publish the edited article. We will replace this Accepted Manuscript with the edited and formatted Advance Article as soon as it is available.

You can find more information about Accepted Manuscripts in the [author guidelines](#).

Please note that technical editing may introduce minor changes to the text and/or graphics, which may alter content. The journal's standard [Terms & Conditions](#) and the ethical guidelines, outlined in our [author and reviewer resource centre](#), still apply. In no event shall the Royal Society of Chemistry be held responsible for any errors or omissions in this Accepted Manuscript or any consequences arising from the use of any information it contains.

Novel high-efficiency visible-light response $\text{Ag}_4(\text{GeO}_4)$ photocatalyst

Xianglin Zhu^a, Peng Wang^{a,*}, Mengmeng Li^b, Qianqian Zhang^a, Elena A. Rozhkova^{c,*}, Xiaoyan Qin^a, Xiaoyang Zhang^a, Ying Dai^b, Zeyan Wang^a, Baibiao Huang^{a,*}

^aState Key Laboratory of Crystal Materials, Shandong University, Jinan 250100,
China

^bSchool of Physics, Shandong University, Jinan 250100, China

^cCenter for Nanoscale Materials, Argonne National Laboratory, Argonne, Illinois
60439, United States

Keywords: Photocatalytic; $\text{Ag}_4(\text{GeO}_4)$; Water splitting; Internal electric field

Abstract

A novel high-efficiency visible-light $\text{Ag}_4(\text{GeO}_4)$ photocatalyst was prepared by a facile hydrothermal method. The photocatalytic activity of as-prepared $\text{Ag}_4(\text{GeO}_4)$ was evaluated by photodegrading of methylene blue (MB) dye and water splitting experiments. The photodegradation efficiency and oxygen production efficiency of $\text{Ag}_4(\text{GeO}_4)$ were detected to be 2.9 and 1.9 times higher than that of Ag_2O . The UV-vis diffuse reflectance spectra (DRS), photoluminescence experiment and photoelectric effect experiments prove that the good light response and high carrier separation efficiency facilitated by the internal electric field is the main reason for $\text{Ag}_4(\text{GeO}_4)$'s excellent catalytic activity. The radical-trapping experiments reveal that photo generated holes are the main active species. First-principles theoretical calculations provide more insight into understanding of the photocatalytic mechanism of $\text{Ag}_4(\text{GeO}_4)$ catalyst.

Introduction

In the past decades, large massive of fossil fuels have been consumed to address needs in energy and chemical products manufacturing for the society development. As a result, global energy crisis and environment pollution issues have become two major thorny issues which must be solved as soon as possible. One efficient approach to resolve these global problems is to use photocatalysis technique, an inherently clean way which can transform inexhaustible energy of solar irradiation into environmentally benign fuels. Photocatalysis has been proved to have promising application in hydrogen generating from water splitting by using of solar energy¹⁻⁴ and organic pollutants' degradation⁵⁻⁷. After years of extensive research efforts toward materials design, synthesis and band-engineering techniques challenges still exist, and industrialization and commercialization of photocatalysts have not yet been realized⁸⁻¹⁴. Hence, the exploring and designing of novel photocatalysts with enhanced performance is required for both the fundamental research and industrial applications.

In order to get photocatalysts with high activity, light absorption ability and efficient carriers' separation efficiency the two main challenges must be solved in the progress of designing and preparing materials. Up to now, visible-light sensitive photocatalysts has been a hot spot in photocatalysis research. Ag-based structures such as Ag@AgX (X=Cl, Br, I), Ag₃PO₄, Ag₂O, Ag₂Mo₃O₁₁ and Ag₂CO₃¹⁵⁻²² have drawn remarkable attention and been considered as one of the most attractive photocatalysts owing to their excellent visible light absorption and high photocatalytic activities in decomposing organic compounds. Besides, the influence of morphology, structure and heterojunction for Ag based photocatalysts were also deeply discussed.³⁵⁻⁴⁰ Due to the special d10 electronic configurations of Ag⁺ ions in AgO-based compounds, the top of valence band (VB) containing the unique hybridized Ag 4d and O2p orbitals can lift the top position of the VB and narrow down the band gap. As a result, these catalysts usually show outstanding visible light absorption properties and excellent photocatalytic activities. Promoting the separation of photogenerated

carriers is also a key point in designing efficient photocatalysts. Most studies on speeding up the rates of charge carriers are mainly focused on construction of heterojunction catalysts, such as $\text{BiPO}_4/\text{Bi}_2\text{WO}_6$, $\text{BiOCl}/\text{BiOBr}$ and $\text{BiPO}_4/\text{BiOI}$ etc.²³ Different from these work, our group²⁴⁻²⁶ and some other researchers²⁷ reported that intrinsic internal electric field covering the whole system is formed within polar materials. The build-in internal electric field plays a critical role in decreasing the recombination of carriers. As a result, Ag-based materials especially with polar structures are considered as new prospective visible-light-driven photocatalysts because of their unique crystal and electronic structures.

Herein, $\text{Ag}_4(\text{GeO}_4)$ was first synthesized through a facile one-step hydrothermal method. The photocatalytic activity of as-prepared sample was characterized by photodegrading MB dye and water splitting in presence of a sacrificial reagent. Our results demonstrate that wide absorption of the visible light and efficient separation of carriers caused by intrinsic internal electric field determine high efficiency of the $\text{Ag}_4(\text{GeO}_4)$ photocatalyst.

Experimental

Synthesis of $\text{Ag}_4(\text{GeO}_4)$ photocatalyst.

Firstly, Na_2GeO_3 was synthesized through solid state reaction method.³⁴ Typically Na_2CO_3 and GeO_2 were grinded together at an equimolar ratio and then pressed into a disk with 1.5 cm-diameter, 5 mm-thick. The disk was heated in air at 900 °C (5°C/min) for 10 hrs and then was grinded into powder for the further use.

$\text{Ag}_4(\text{GeO}_4)$ was synthesized through a simple one-step hydrothermal method. In details, 10.0 mmol AgNO_3 and 2.5 mmol Na_2GeO_3 were dissolved in 40 mL deionized water. Then the Na_2GeO_3 solution was dropped into AgNO_3 solution slowly under vigorous stirring. After stirring for three hours, the mixed solution was transferred into 100 mL Teflon-lined autoclaves, which were sealed at 120°C for 10 h and then cooled down naturally. Precipitate was filtered through a filter membrane and washed with deionized water and absolute ethanol for three times and then dried

at 60°C for 2h.

Ag₂O was synthesized by the similar solid state method as Ag₄(GeO₄), only replacing Na₂GeO₃ with 10 mmol NaOH.

Bulk g-C₃N₄ was obtained by heating melamine at 550 °C with a ramp rate of 2 °C/min for 4 h.

Characterization

The structure of Ag₄(GeO₄) was characterized by X-ray diffraction (XRD) using Bruker AXS D8 advance powder diffractometer (Cu K α X-ray radiation, $\lambda=0.154056$ nm). The morphologies of as-prepared samples were characterized using scanning electron microscopy (SEM, Hitachi S4800). UV-Vis diffuse reflectance spectra were recorded using a Shimadzu UV 2550 spectrophotometer equipped with an integrating sphere; and BaSO₄ was used as a reference. PLS-SXE 300, Beijing Trusttech Co. Ltd 300 W Xe arc lamp equipped with an ultraviolet cutoff filter ($\lambda > 420$ nm, 85 mW/cm²) was used as visible-light source. The amount of produced O₂ was determined with a gas chromatograph (Varian GC-3800) equipped with thermal conductivity detector and 5 Å molecular sieve column.

Photocatalytic experiments

The photocatalytic activities of as-prepared samples were evaluated through the degrading MB dye and photocatalytic oxygen generation under visible light irradiation ($\lambda > 420$ nm). Typically, 50 mg photocatalyst was dispersed in 50 mL MB dye solution (20 mg/L in deionized water), and the suspension was stirred and kept in dark for half an hour to attain adsorption saturation. Then, photocatalytic experiment was carried out under irradiation of 300 W Xe arc lamp. 3 mL of the mixed suspension was taken every 10 minutes and centrifuged to remove solid photocatalyst. The residual organic dye solutions were analyzed using a UV-vis spectrophotometer. Photocatalytic production of oxygen was carried out in presence of AgNO₃. Typically, 100 mg photocatalyst was added into 100 mL of aqueous AgNO₃ solution (0.015 M), which was kept at 20°C in a quartz reactor. The reactor

was sealed and vacuumed in order to remove the residual oxygen and switched on the 300 W Xe lamp. The output of oxygen was detected every half an hour.

Results and discussion

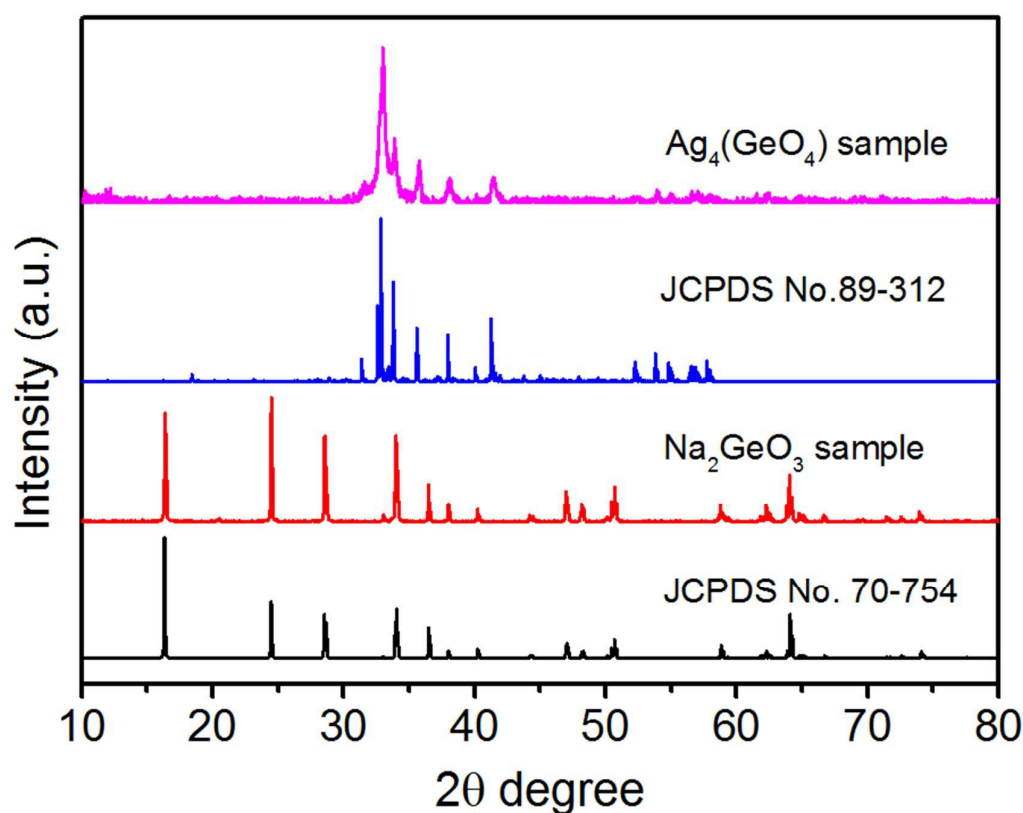


Fig. 1. XRD patterns of the as-synthesized Na_2GeO_3 and $\text{Ag}_4(\text{GeO}_4)$.

The crystal structures of as-prepared Na_2GeO_3 and $\text{Ag}_4(\text{GeO}_4)$ were characterized by XRD. As it can be seen from the Fig. 1, the peaks of synthesized raw material Na_2GeO_3 are in well accordance with the peaks of the standard card. Peaks of neither side products nor initial materials were detected, revealing purity of the synthesized Na_2GeO_3 . The peaks of synthesized $\text{Ag}_4(\text{GeO}_4)$ also exactly correspond to the standard card (JPCDS No.89-312).

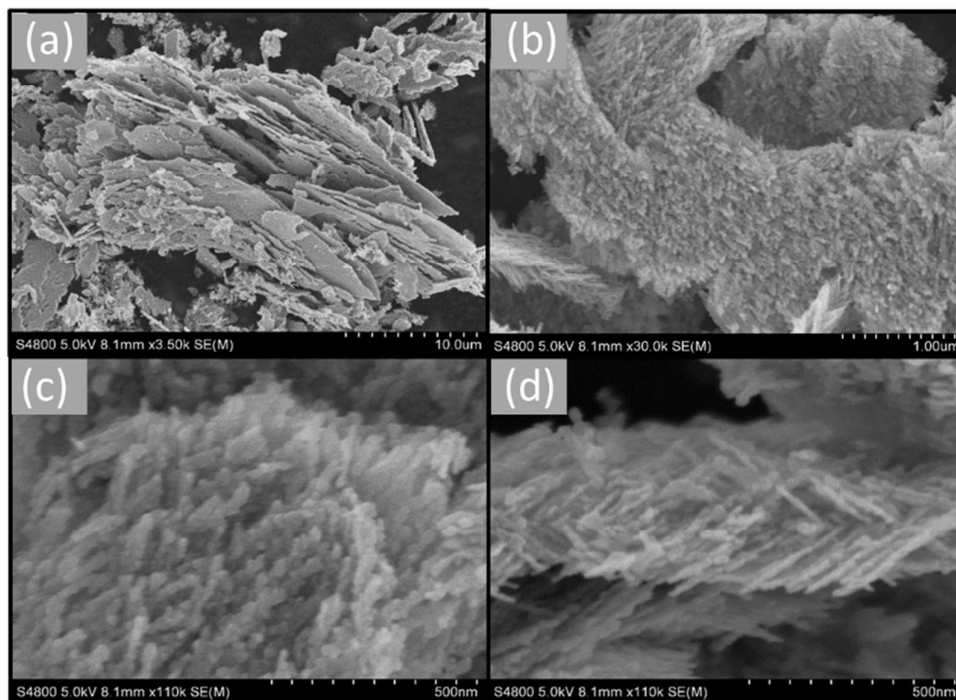


Fig. 2. SEM images of the as-synthesized $\text{Ag}_4(\text{GeO}_4)$: (a), (b) low magnification and (c),(d) high magnification SEM images.

The morphology of as-prepared $\text{Ag}_4(\text{GeO}_4)$ photocatalyst was characterized by scanning electron microscopy (SEM), as shown in Fig. 2. Lower magnification SEM images (Fig. 2a and b) show that the prepared $\text{Ag}_4(\text{GeO}_4)$ samples represent irregularly sized carpet-looking microfilms. The higher magnification SEM images (Fig. 2c and d) demonstrate that these ~ 300 nm-thick films are composed of uniform criss-crossing nanorods.

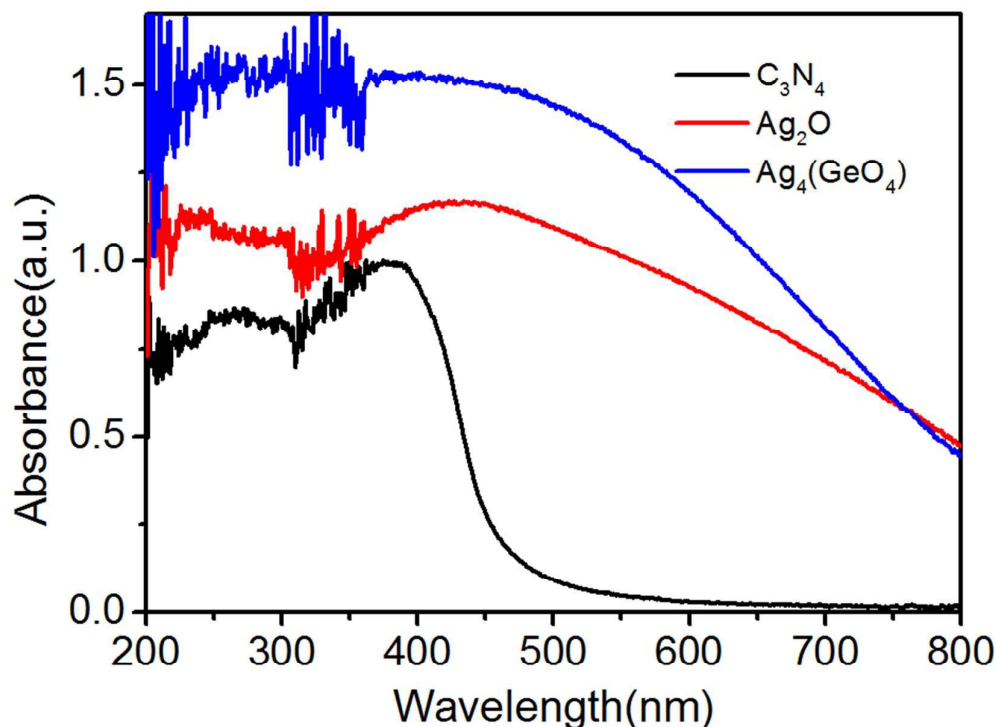


Fig. 3. UV-vis diffuse reflectance spectra (DRS) of Ag₄(GeO₄), Ag₂O and C₃N₄.

The optical properties of as-prepared Ag₄(GeO₄), Ag₂O and C₃N₄ samples were studied using UV-vis diffuse reflectance spectra (DRS). As shown in Fig. 3, both Ag₄(GeO₄) and Ag₂O demonstrate better performance in light absorbance compared with C₃N₄. While Ag₄(GeO₄) shows lower absorption in visible light region than Ag₂O, it still covers the 200-800nm UV-visible light region. Efficient absorption in visible light region is propitious for enhancing photoexcitation efficiency consequently leading to higher photocatalytic activity.

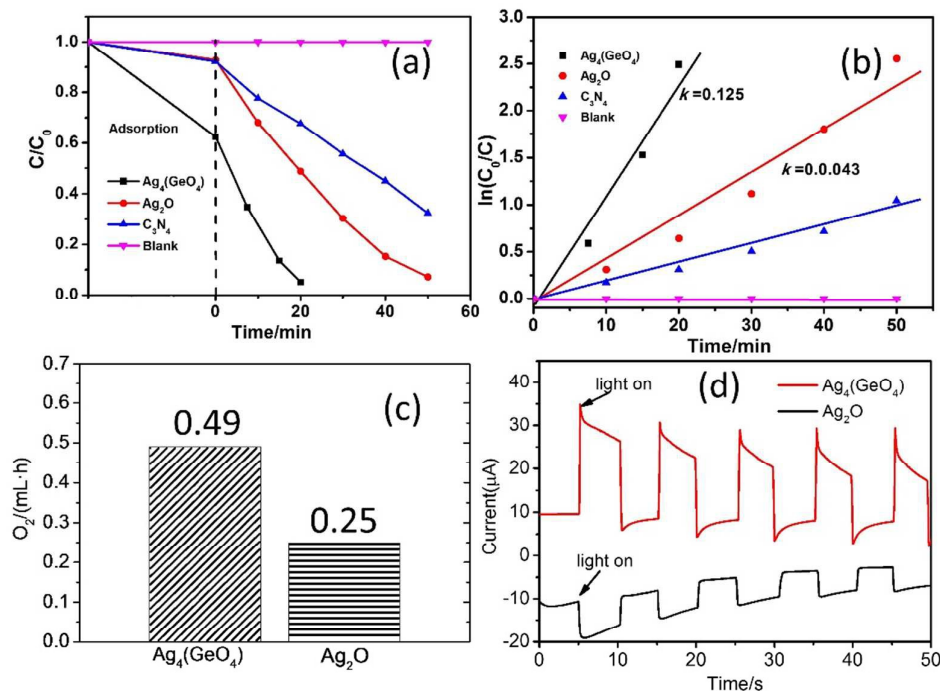


Fig. 4. (a),(b) Photo-degradation of MB dye solutions under visible light irradiation ($\lambda > 420$ nm, 85 mW/cm^2), (c) Photocatalytic O_2 production from water under visible light irradiation ($\lambda > 420$ nm), (d) Photocurrent results of $\text{Ag}_4(\text{GeO}_4)$ and Ag_2O ($\lambda > 420$ nm).

Photocatalytic performance of as-prepared samples was evaluated by photodegradation of methylene blue (MB) solution, photocatalytic O_2 generation and photocurrent response under visible light irradiation (Fig. 4). As presented in Fig. 4a and b both $\text{Ag}_4(\text{GeO}_4)$ and Ag_2O can bleach MB solution more efficiently than C_3N_4 . $\text{Ag}_4(\text{GeO}_4)$ sample showed the best performance, and over 95% of the dye was removed within 20 min. The $\ln(C_0/C)$ -time curves of the three catalysts excluding the effect of adsorption also prove that $\text{Ag}_4(\text{GeO}_4)$ has the highest reaction rate and the degradation rate of $\text{Ag}_4(\text{GeO}_4)$ is 2.9 times that of Ag_2O .

In photocatalytic water splitting experiments (Fig. 4c), similar tendencies were observed, water splitting over the $\text{Ag}_4(\text{GeO}_4)$ catalysts resulted in higher oxygen yield than over the Ag_2O under the same conditions. The oxygen generation rate of $\text{Ag}_4(\text{GeO}_4)$ is 1.9 times that of Ag_2O . In order to further understand the reasons of

better performance of $\text{Ag}_4(\text{GeO}_4)$, the photoelectrochemical properties of $\text{Ag}_4(\text{GeO}_4)$ and Ag_2O samples were compared. The photocurrent measurements results shown in Fig. 4d demonstrate that $\text{Ag}_4(\text{GeO}_4)$ has higher photocurrent response than that of Ag_2O , indicating that more electrons and holes are generated and separated under the visible light irradiation. BET surface area of $\text{Ag}_4(\text{GeO}_4)$, Ag_2O and C_3N_4 was also characterized. Compared with the BET surface area of Ag_2O and C_3N_4 ($5.4 \text{ m}^2/\text{g}$ and $14.0 \text{ m}^2/\text{g}$), $\text{Ag}_4(\text{GeO}_4)$ has the biggest BET surface area of $18.8 \text{ m}^2/\text{g}$ and this is one of the reasons that $\text{Ag}_4(\text{GeO}_4)$ shows best activity.

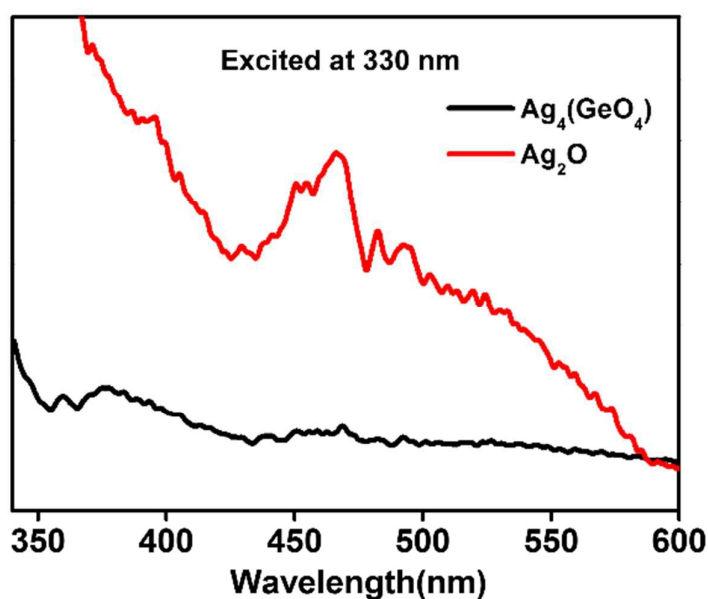


Fig. 5. Photoluminescence experiment of $\text{Ag}_4(\text{GeO}_4)$ and Ag_2O .

From photoluminescence spectra, the recombination rates of electron-hole pairs in photocatalysts can be evaluated. Typically, the higher PL intensity means the higher recombination of electron hole pair. Fig. 5 is the PL spectra of $\text{Ag}_4(\text{GeO}_4)$ and Ag_2O excited at 330 nm. $\text{Ag}_4(\text{GeO}_4)$ and Ag_2O have weak PL intensity, while $\text{Ag}_4(\text{GeO}_4)$ has lower intensity than Ag_2O . This indicates the better separation efficiency of carriers in $\text{Ag}_4(\text{GeO}_4)$.

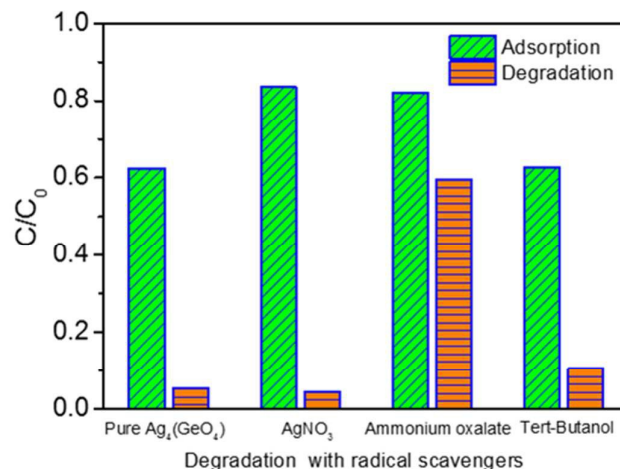


Fig. 6. Photocatalytic experiments in presence of ammonium oxalate, AgNO₃, tert-butanol respectively under visible light irradiation ($\lambda > 420$ nm).

Hydroxyl radicals $\cdot\text{OH}$ have been identified among few typical reactive species to be involved into photocatalytic degradation of organic dyes²⁸. Therefore, to identify the major reactive species involved into photodegradation of MB solution over the Ag₄(GeO₄) catalyst, radical-trapping experiments were carried out using ammonium oxalate, AgNO₃ and tert-butanol as hole-, electron- and $\cdot\text{OH}$ radical - scavengers (respectively) under identical conditions. As shown in Fig. 6, adsorption changed after adding of these radical scavengers. Degradation efficiencies didn't change noticeably in presence of AgNO₃ and tert-butanol compared to pure Ag₄(GeO₄), proposing that electrons and $\cdot\text{OH}$ radicals are not the main reactive species during the MB degradation. However, when ammonium oxalate was added, the photocatalytic activity of Ag₄(GeO₄) was greatly suppressed, indicating that the photogenerated holes were the major reactive species involved into the MB photodegradation.

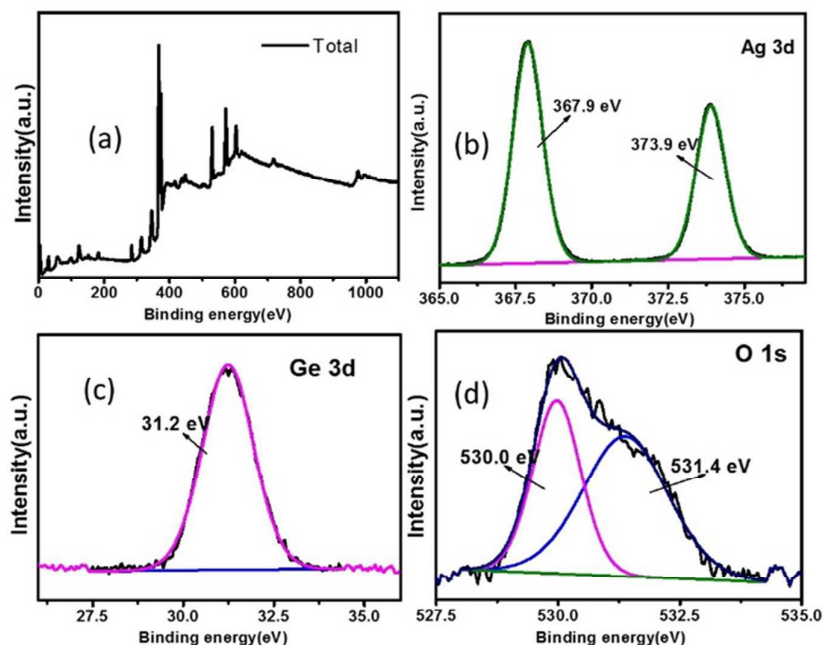


Fig. 7. XPS results of the as-prepared $\text{Ag}_4(\text{GeO}_4)$.

The chemical valence states and surface compositions of $\text{Ag}_4(\text{GeO}_4)$ have been investigated, as shown in Fig. 7. Fig. 7 (a) is the full XPS survey scan of $\text{Ag}_4(\text{GeO}_4)$ which exhibits the characteristic peaks of Ag, Ge and O. The high resolution XPS of Ag 3d, Ge 3d and O 1s are shown in Fig. 7b, c and d. Two peaks at 367.9 eV and 373.9 eV corresponded to characteristic peaks of Ag^+ in $\text{Ag}_4(\text{GeO}_4)$ ²⁹. No Ag^0 was detected in XPS test. Signals around the 31.2 eV are the Ge 3d characteristic peaks.³⁰ Two peaks at about 530.0 eV and 531.4 eV corresponded to signals of O1s crystal O element and adsorption O element.³¹

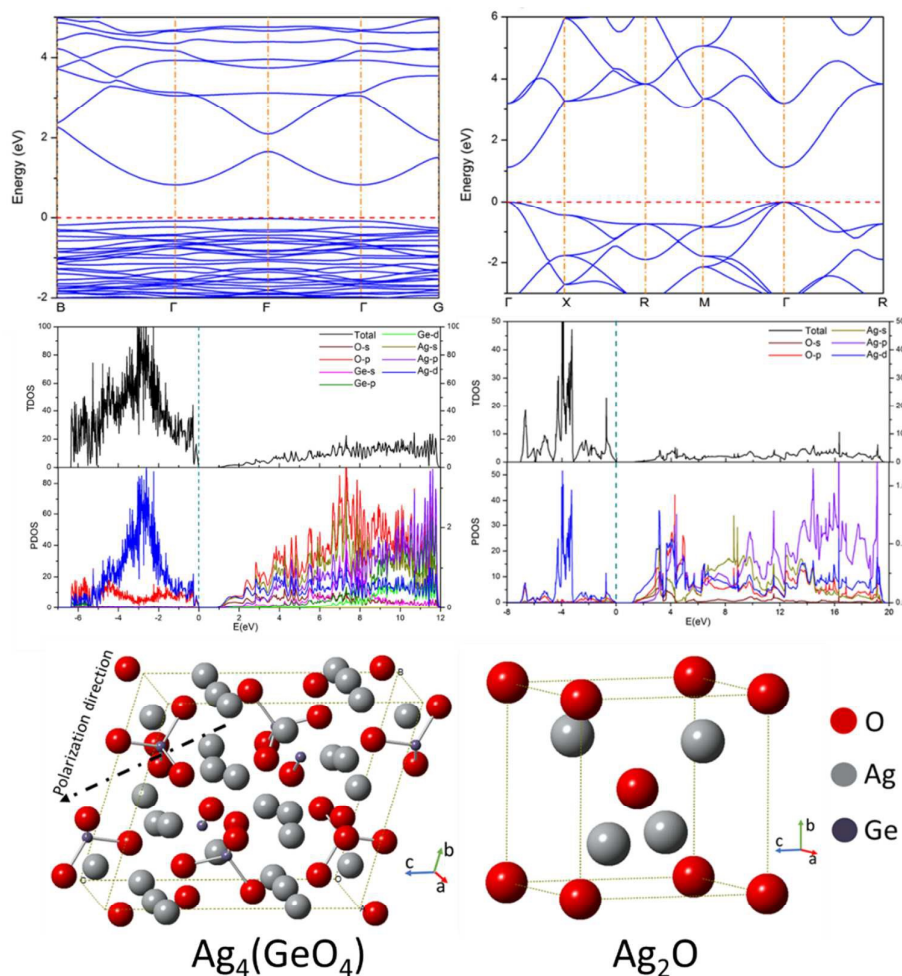


Fig. 8. Energy band diagram, DOS calculation results, crystal structure of $\text{Ag}_4(\text{GeO}_4)$ and Ag_2O and polarization direction of $\text{Ag}_4(\text{GeO}_4)$.

In order to get further insight into the mechanism of photo excitation and separation of photogenerated electrons and holes, the energy band diagrams, DOS diagrams and crystal structures of $\text{Ag}_4(\text{GeO}_4)$ and Ag_2O were produced using DFT calculation methods,(Fig. 8). As it can be seen from total DOS and local DOS, the top of valence band of $\text{Ag}_4(\text{GeO}_4)$ is mainly consisted of hybridized Ag 4d and O2p states and the bottom of conduction band is majorly formed with Ag 5s and Ag 4d states, which are very similar to the results of Ag_2O . As it follows from the calculations, in the $\text{Ag}_4(\text{GeO}_4)$ crystal Ge element does little contribution to construction of $\text{Ag}_4(\text{GeO}_4)$'s VB and CB. Similarly to Ag_2O the unique d10 and sp/p configurations are the main

reason for the visible light absorption of $\text{Ag}_4(\text{GeO}_4)$.^{32, 33} In view of another key factor influencing the photocatalytic properties, the separation efficiency of photo-generated carriers is the vital factor that determines the photocatalytic performance of $\text{Ag}_4(\text{GeO}_4)$. As for $\text{Ag}_4(\text{GeO}_4)$ crystal, there is no symmetric center exists because of the non-symmetric Ge-O tetrahedron present in the structure. As a result, an intrinsic internal electric field covering the whole material forms and promotes the separation of photogenerated carriers. The latter results in more separated holes available to join the oxidation reaction under irradiation of visible light.

Based on all the experimental and calculation results, we propose a possible mechanism which can explain the high photocatalytic activity of $\text{Ag}_4(\text{GeO}_4)$ photocatalyst. Under the irradiation of visible light, electrons and holes are generated and join the photocatalytic reaction. More carriers could be separated owing to the existing intrinsic internal electric field in the $\text{Ag}_4(\text{GeO}_4)$ crystal. As a result, more photo-generated holes can be separated and, consequently, get involved into the photocatalytic reaction, that leads to higher activities of $\text{Ag}_4(\text{GeO}_4)$ compared with Ag_2O .

Conclusion

A novel photocatalytic material $\text{Ag}_4(\text{GeO}_4)$ was synthesized for the first time through a hydrothermal method. The photocatalytic activities of the as-prepared $\text{Ag}_4(\text{GeO}_4)$ were evaluated through photo-degradation of MB dye solution and photocatalytic O_2 evolution. $\text{Ag}_4(\text{GeO}_4)$ photocatalyst showed excellent visible light photocatalytic activities compared with Ag_2O photocatalyst. Both the experiments and calculations results demonstrate that the wide range of light absorption and higher separation of generated holes and electrons are the main reason that $\text{Ag}_4(\text{GeO}_4)$ has advanced performance. Compared to Ag_2O photocatalyst, there is intrinsic internal electric field formed in the $\text{Ag}_4(\text{GeO}_4)$ arising from the polar structure that promotes separation of photogenerated electrons and holes. As a result, the $\text{Ag}_4(\text{GeO}_4)$ shows higher photo-oxidation abilities. Our new results provide further guidance for the

designing of advanced high efficiency photocatalysts.

Acknowledgements

This work was financially supported by a research Grant from the National Basic Research Program of China (No. 2013CB632401), the National Natural Science Foundation of China (No. 21333006, 21573135, 11374190 and 51602179), Recruitment Program for Young Professionals, China, Taishan Scholar Foundation of Shandong Province, China. Dr. Rozhkova was supported by the U.S. Department of Energy, Office of Science, Office of Basic Energy Sciences, contract no. DE-AC02-06CH11357.

Notes and references

- (1) A. Fujishima, K. Honda, *Nature*, 1972, 238, 37–38.
- (2) A. Kubacka, M. Fernández-García, G. Colón, *Chem. Rev.*, 2012, 112, 1555–1614.
- (3) D.J. Martin, P.J. Reardon, S.J. Moniz, J. Tang, *J. Am. Chem. Soc.*, 2014, 136, 12568–12571.
- (4) J. Zhao, Y. Wang, Y.X. Li, X. Yue and C.Y. Wang, *Catal. Sci. Technol.*, 2016, 6, 7967-7975
- (5) L. Liu, Y.H. Qi, J.S. Hu, W.J. An, S.L. Lin, Y.H. Liang and W.Q. Cui, *Materials Letters*, 2015, 158, 278-281.
- (6) D. Liu, M. W. Zhang, W. J. Xie, L. Sun, Y. Chen and W. W. Lei, *Catal. Sci. Technol.*, 2016, 6, 8309-8313.
- (7) J.H. Yang, J. Wang, X.Y. Li, D.D. Wang and H. Song, *Catal. Sci. Technol.*, 2016, 6, 4525-4534.
- (8) D. P. DePuccio and C. C. Landry, *Catal. Sci. Technol.*, 2016, 6, 7512-7520.
- (9) W.-K. Jo, T.S. Natarajan, *Chem. Eng. J.*, 2015, 281, 549–565.
- (10) J. Pan, J. Li, Z. Yan, B. Zhou, H. Wu, X. Xiong, *Nanoscale*, 2013, 5, 3022–3029.
- (11) Y. Wu, M. Xu, X. Chen, S. Yang, H. Wu, J. Pan, X. Xiong, *Nanoscale*, 2015, 8, 440–450.

- (12) M. Wu, J.M. Yan, X.W. Zhang, M. Zhao, Q. Jiang, *J. Mater. Chem. A*, 2015, 3, 15710–15714.
- (13) M.M. Rahman, S.B. Khan, A. Jamal, M. Faisal, A.M. Asiri, *Chem. Eng. J.*, 2012, 192, 122–128.
- (14) F.T. Chen, Z. Liu, Y. Liu, P.F. Fang, Y.Q. Dai, *Chem. Eng. J.*, 2013, 221, 283–291.
- (15) P. Wang, B.B. Huang, X.Y. Qin, X.Y. Zhang, Y. Dai, *Angew. Chem. Int. Ed.*, 2008, 47, 7931–7933.
- (16) K. Awazu, M. Fujimaki, C. Rockstuhl, J. Tominaga, H. Murakami, Y. Ohki, N. Yoshida, *J. Am. Chem. Soc.*, 2008, 130, 1676–1680.
- (17) Z.Y. Chen, L. Fang, W. Dong, F.G. Zheng, M.T. Shen, J.L. Wang, *J. Mater. Chem. A*, 2014, 2, 824–832.
- (18) Y.Y. Wen, H.M. Ding, Y.K. Shan, *Nanoscale*, 2011, 3, 4411–4417.
- (19) P. Wang, B.B. Huang, X.Y. Zhang, X.Y. Qin, H. Jin, Y. Dai, Z.Y. Wang, M-H. Whangbo, *Chem. Eur. J.*, 2009, 15, 1821–1824.
- (20) X.F. Wang, S.F. Li, H.G. Yu, J.G. Yu, S.W. Liu, *Chem. Eur. J.*, 2011, 17, 7777–7780.
- (21) J.T. Tang, Y.H. Liu, H.Z. Li, Z. Tan, D.T. Li, *Chem. Commun.*, 2013, 49, 5498–5500.
- (22) Z.G. Yi, J.H. Ye, N. Kikugawa, T. Kako, S.X. Ouyang, H. Yang, J.Y. Cao, W.J. Luo, Z.S. Li, Y. Liu, *Nat. Mater.*, 2010, 9 (7), 559–564.
- (23) Y.Y. Zhu, Y.J. Wang, Q. Ling, Y.F. Zhu, *Appl. Catal. B: Environ.*, 2017, 200, 222–229; X.M. Jia, J. Cao, H.L. Lin, M. Y. Zhang, X.M. Guo, S.F. Chen, *Appl. Catal. B: Environ.*, 2017, 204, 505–511; Y.F. Liu, W.Q. Yao, D. Liu, R.L. Zong, M. Zhang, X. G. Ma, Y.F. Zhu, *Appl. Catal. B: Environ.*, 2015, 163, 547–553.
- (24) X.L. Zhu, P. Wang, B.B. Huang, X.C. Ma, Y. Dai *Appl. Catal. B: Environ.*, 2016, 199, 315–322.
- (25) Z.Z. Lou, B.B. Huang, Z.Y. Wang, X.C. Ma, X.Y. Zhang, X.Y. Qin, Y. Dai, M.-H. Whangbo, *Chem. Mater.*, 2014, 26, 3873–3875.
- (26) W.J. Wang, B.B. Huang, Z.Y. Wang, X.C. Ma, X.Y. Zhang, X.Y. Qin, Y. Dai, M-H.

- Whangbo, *Chem. Eur. J.*, 2013, 19, 14777–14780.
- (27) J. Li, L.J. Cai, J. Shang, Y. Yu, L.Z. Zhang, L. Z, *Adv. Mater.*, 2016, 28, 4059-4064.
- (28) H.P. Li, J.Y. Liu, W.G. Hou, N. Du, R.J. Zhang, X.T. Tao, *Appl. Catal. B: Environ.*, 2014, 160–161, 89–97.
- (29) X.H. Wang, J. Yang, S.Q. Ma, D. Zhao, J. Dai and D.F. Zhang, *Catal. Sci. Technol.*, 2016, 6, 243-253.
- (30) R. Wang, S.p. Wu, Y.C. Lv, and Z. Q. Lin, *Langmuir*, 2014, 30, 8215–8220.
- (31) S. Kim, C. Kim, J.-Y. Hong, S. H. Hwang, J. Jang, *RSC Adv.*, 2014, 4, 6821–6824.
- (32) H.J. Dong, G. Chena, J.X. Sun, C.M. Li, Y.G. Yu, D.H. Chen, *Appl. Catal. B: Environ.*, 2013, 134 – 35, 46– 54.
- (33) A. Al-keisy, L. Ren, D.D. Cui, Z.F. Xu, X.Xu, X.D. Su, W.C. Hao, Y. Du, *J. Mater. Chem. A*, 2016, 4, 10992–10999.
- (34) N. Zhang, S.X. Ouyang, P. Li, Y.J. Zhang, G.C. Xi, T. Kako and J.H. Ye, *Chem. Commun.*, 2011, 47, 2041-2043.
- (35) Z.-H. Yang, C.-H. Ho, S. Lee, *Appl. Surf. Sci.*, 2015, 394, 609-614.
- (36) D.H. Cui, Y.F. Zheng, X.C. Song, *J. Alloys Compd.*, 2017, 701, 163-169.
- (37) S.B. Yang, D.B. Xu, B.Y. Chen, B.F. Luo, X. Yan, L.S. Xiao, W.D. Shi, *Appl. Surf. Sci.*, 2016, 383, 214-221.
- (38) Y.Q. Cui, Q.L. Ma, X.Y. Deng, Q. Meng, X.W. Chenga, M.Z. Xie, X.L. Li, Q.F. Cheng, H.L. Liu, *Appl. Catal. B: Environ.*, 201, 206, 136-145.
- (39) H.Q. Wang, J.Z. Li, P.W. Huo, Y.S. Yan, Q.F. Guan, *Appl. Surf. Sci.*, 2016, 366, 1-8.
- (40) S.X. Ouyang, N. Kikugawa, Z.G. Zou, J.H. Ye, *Appl. Catal. A*, 2009, 366, 309-314.

The exiting of internal electric field promotes the separation of generated carriers, enhances the photocatalytic activity in the polar materials

TOC Graphic

